Materials Letters 230 (2018) 123–127

Contents lists available at ScienceDirect

Materials Letters

journal homepage: www.elsevier.com/locate/mlblue

Hierarchical porous carbon materials from bio waste-mango stone for high-performance supercapacitor electrodes

Xiaoli Su, Shuai Jiang, Xiucheng Zheng *, Xinxin Guan, Pu Liu, Zhikun Peng *

College of Chemistry and Molecular Engineering, Zhengzhou University, Zhengzhou 450001, China

ARTICLE INFO

Article history:
Received 6 April 2018
Received in revised form 7 July 2018
Accepted 23 July 2018
Available online 24 July 2018

Keywords:
Mango stone
Carbon materials
Hierarchical pores
Electrical properties
Supercapacitor

ABSTRACT

Porous activated carbon was successfully fabricated from bio waste-mango stone via a two-step chemical etching strategy. The optimized carbon material (denoted as MGKZ-2) displayed a high specific capacitance of 353.8 F g^{-1} at 0.5 A g^{-1} and a satisfactory rate capability in the three-electrode supercapacitor system. Moreover, MGKZ-2-based symmetric cell presented a high energy density of 27.6 Wh kg^{-1} at 159.9 W kg^{-1}, as well as long-term cycling stability due to its hierarchical pores to offer large ion-accessible surface area, efficient ion diffusion and electron transport pathways.

© 2018 Elsevier B.V. All rights reserved.

1. Introduction

Among numerous available energy storage technologies, electrochemical capacitors are attractive because of their high power density, good rate capability, and long cycling life [1,2]. As one possible resource of carbons served as electricial double layer capacitors (EDLCs) electrode materials, biomass has unique advantages including easy availability, low cost, renewability and friendly to the environment [3–5]. Additionally, biomass-derived carbon materials inherit both the structural flexibility and chemical diversity of the natural resources, which can facilitate improving capacitive performance.

Mango is a common fruit and a large amount of bio waste-mango stone is generated. Herein, we adopt a two-step etching approach to fabricate porous carbons. The exciting results demonstrate an efficient way for preparing high-performance supercapacitor electrode materials.

2. Experimental methods

Mango stone was washed with deionized (DI) water, dried at 100 °C, calcined at 300 °C for 10 min and grinded into powders. As shown in Fig. S1, 2 g of mango stone powder was immersed with $ZnCl_2$ solution and then rapidly frozen by liquid nitrogen. The resultant ice crystals prevented the aggregation of mango stone particles. After freeze-drying, the solid was calcined at 600 °C for 4 h with a ramp rate of 3 °C min^{-1} under N_2 atmosphere and treated with HCl solution (1.0 mol L^{-1}) at 90 °C. After washing with DI water and drying at 110 °C, the product was further impregnated with KOH solution (2 mol L^{-1}) with a mass ratio of 4:1 (KOH:the resultant solid), followed by evaporating water at 80 °C and calcined at 800 °C for 1 h with a heat rate of 3 °C min^{-1} under N_2 atmosphere. Then, the solid was treated with HCl solution and washed with DI water. The resultant carbon was denoted as MGKZ-*x*, where *x* represented the mass ratio of $ZnCl_2$ to mango stone powder (*x* = 1, 2, 3, and 4, respectively).

For comparison, mango stone powders were directly calcined at 600 °C for 4 h under N_2 atmosphere and the as-prepared material was denoted as MG. MG was further activated with KOH and treated as that for the aforementioned MGKZ-*x*, and the resultant carbon was denoted as MGK.

The samples were characterized by various techniques and the capacitive performance was investigated using a three-electrode system. The electrochemical performance of MGKZ-2 was further investigated in a symmetric supercapacitor. The detailed information was offered in Supplementary Material.

3. Results and discussion

As shown in Fig. 1a and b, MG exhibits an assembled hollow individual tubular-like structure with a rough surface. Compared with MG without obvious pores (Fig. 1c) and MGK with many flake brittle fragments formed by the KOH etching (Fig. 1d), MGKZ-2

* Corresponding authors.
E-mail addresses: zhxch@zzu.edu.cn (X. Zheng), zhikunpeng@163.com (Z. Peng).

https://doi.org/10.1016/j.matlet.2018.07.096
0167-577X/© 2018 Elsevier B.V. All rights reserved.

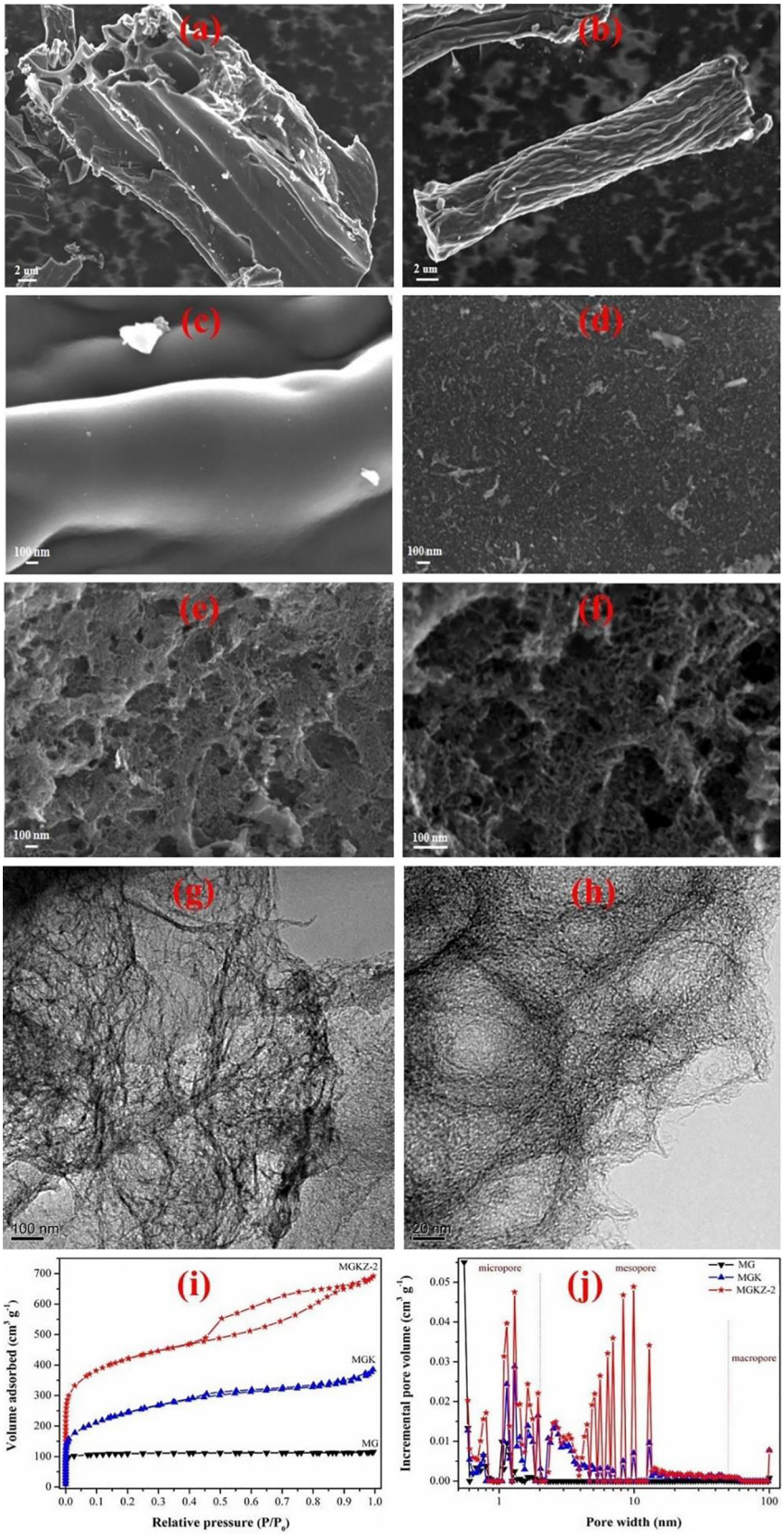

Fig. 1. SEM images of MG (a–c), MGK (d) and MGKZ-2 (e, f); TEM images of MGKZ-2 (g, h); N_2 adsorption-desorption isotherms (i) and pore size distribution curves (j) of MG, MGK and MGKZ-2.

exhibits an interconnected porous structure (Fig. 1e and f), which is also confirmed by its TEM images shown in Fig. 1g and h. The porous structure may be served as ion channels to promote the ion transmission and diffusion kinetics [6]. Their textural structures are further investigated by N_2 adsorption-desorption measurement. As shown in Fig. 1i and j, MG show the type I

isotherm while MGK and MGKZ-2 exhibit the typical IV isotherms. Moreover, the obvious steep raise of N_2 uptake at low relative pressures ($P/P_0 < 0.1$) reveal the existence of micropores [7]. The pore size distribution curves reveal that both MGKZ-2 and MGK exhibit a wide distribution in the range of 0–70 nm, while MG has a relatively narrow distribution (0–2 nm). As summarized in Table S1, MGKZ-2 possesses a specific surface area (S_{BET}) of 1497.8 $m^2 g^{-1}$ and a total pore volume (V_p) of 1.070 $cm^3 g^{-1}$, which are much higher than those of MGK (S_{BET} = 839.4 $m^2 g^{-1}$, V_p = 0.596 $cm^3 g^{-1}$) and MG (S_{BET} = 393.7 $m^2 g^{-1}$, V_p = 0.178 $cm^3 g^{-1}$). The hierarchical structure of MGKZ-2 is perfect for supercapacitor electrode because the charge accumulation happens primarily in micropores, whereas the mesopores can transfer abundant electrolytes to and from the micropores, improving the utilization of the micropores. Meanwhile, macropores can play the role of ion-buffering reservoirs to store more electrolyte ions [8].

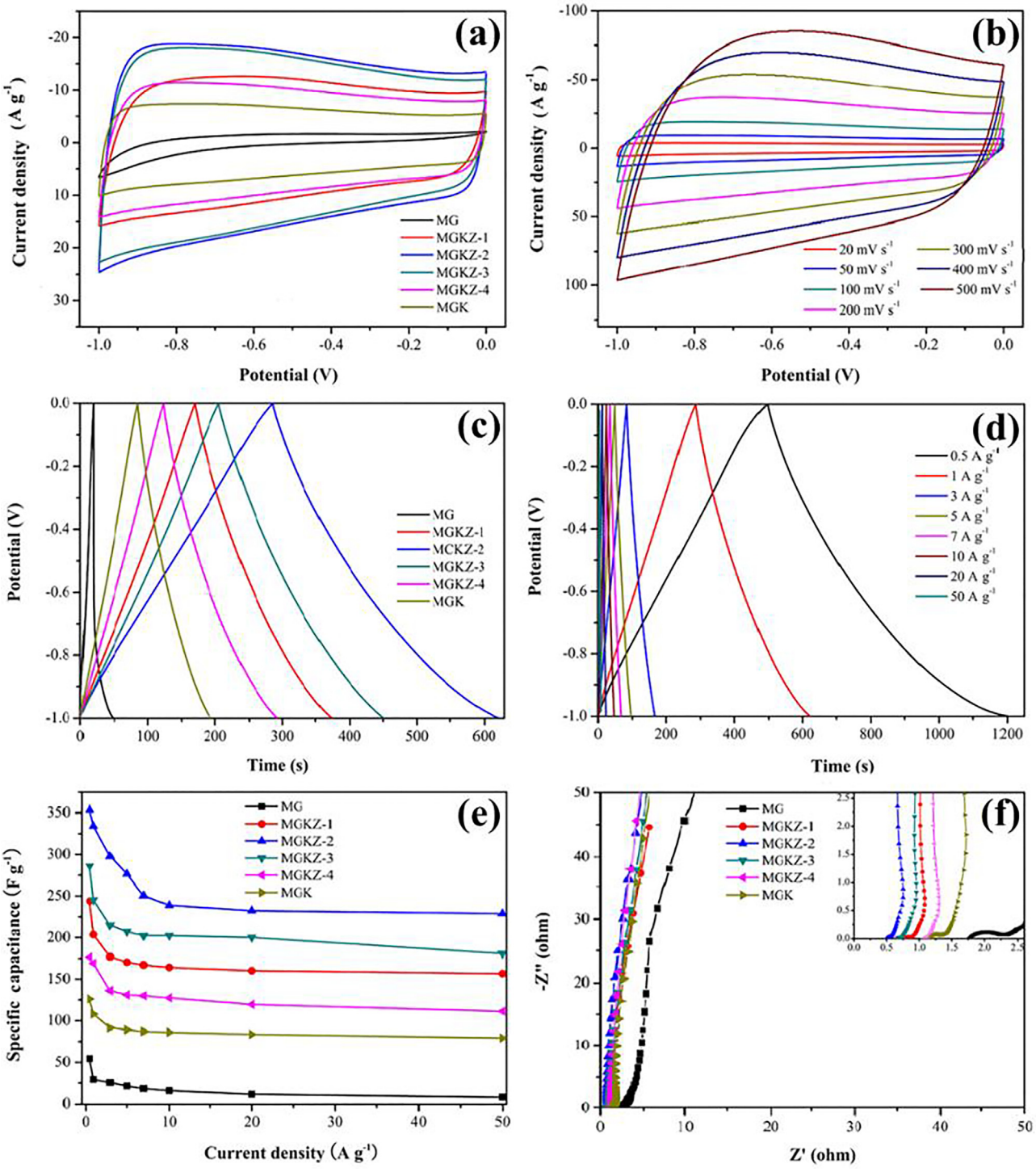

Fig. 2. Electrochemical performances of MG, MGK, and MGKZ-*x* in the three-electrode system: (a) CV curves for MG, MGK, and MGKZ-*x* at 100 mV s^{-1}; (b) CV curves of MGKZ-2 at various scan rates; (c) GCD curves of MG, MGK, and MGKZ-*x* at 1 A g^{-1}; (d) GCD curves for MGKZ-2 at different current densities; (e) Specific capacitances of MG, MGK, and MGKZ-2 at different current densities; and (f) Nyquist plots for MG, MGK, and MGKZ-*x*.

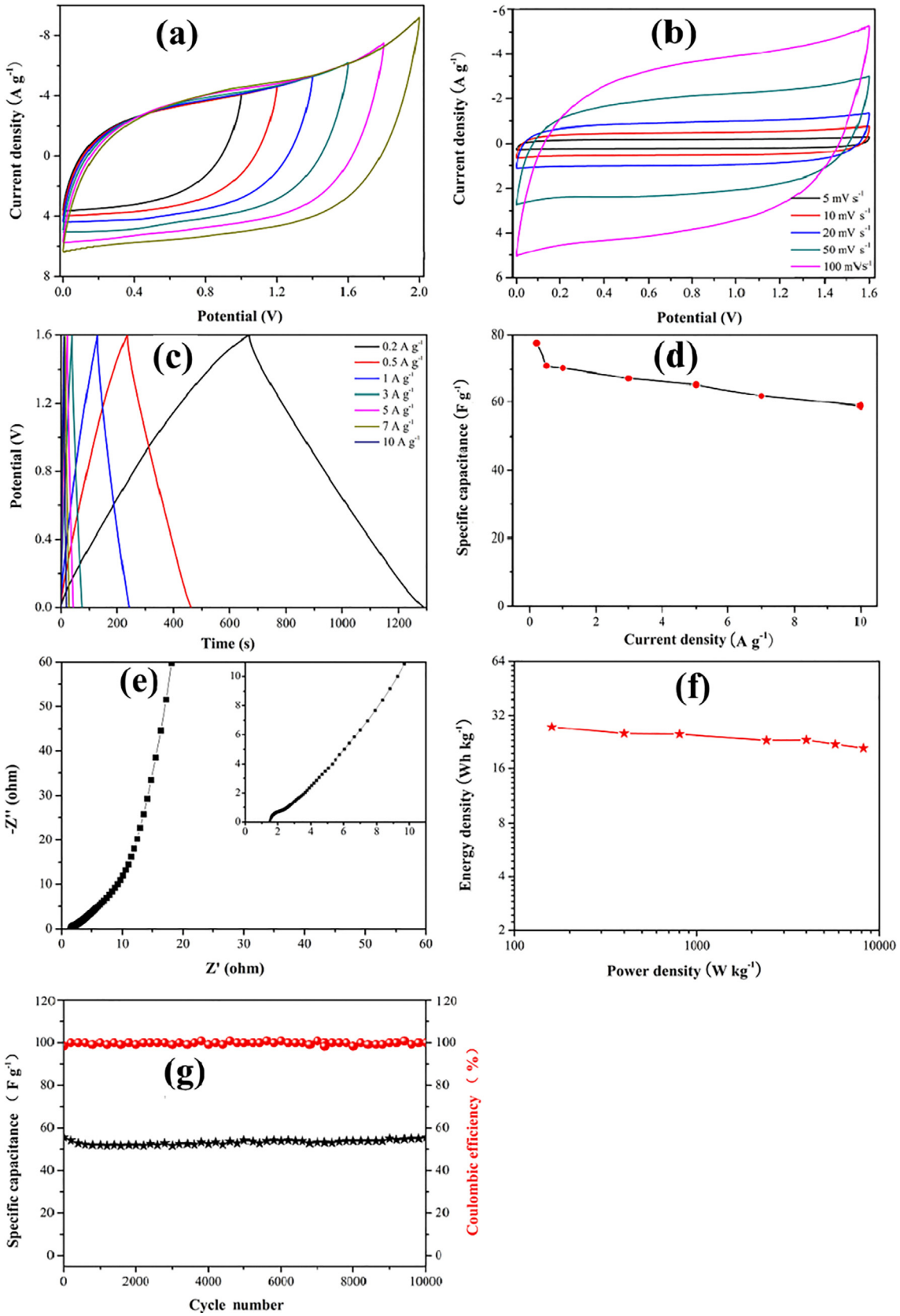

Fig. 3. Electrochemical performance of MGKZ-2 in the symmetrical system: (a) CV curves at 100 mV s^{-1}; (b) CV curves at various scan rates; (c) GCD curves at different current densities; (d) Specific capacitances at different current densities; (e) Nyquist plots; (f) The Ragone plots; and (g) The specific capacitance and columbic efficiency at 10 A g^{-1}.

A broad peak at 22.5° and a weak one at 43.0°, which are ascribed to the (0 0 2) and (1 0 0) planes of graphitic carbon, respectively, appear in all the XRD patterns (Fig. S2). The peak intensity of MGK and MGKZ-2, especially for that of (0 0 2), are obviously lower than that of MG, indicating the improvement of graphitization degree.

The XPS survey spectrum shows three major peaks centering at 284.8, 401.0 and 533.0 eV corresponded to C 1s, N 1s and O 1s, respectively (Fig. S4a). The oxygen and nitrogen-functional groups can improve the wettability of the electrolyte, resulting in the efficient utilization of the surface area, and improving ion transport properties at high current densities.

All the cyclic voltammetry (CV) measurements of the carbon materials in the three-electrode supercapacitor system shown in Fig. 2a reveal nearly rectangular shape with rapid current response, indicating they have good EDLC feature. Moreover, the CV curves for MGKZ-*x* exhibit larger area than those of MG and MGK, implying they have higher specific capacitances. Among MGKZ-*x*, MGKZ-2 gives the highest specific capacitance. As shown in Fig. 2b, even at 500 mV s^{-1}, the rectangular symmetry CV curve for MGKZ-2 is still maintained. Compared with MG, which exhibits a non-linear galvanostatic charge/discharge (GCD) curve (Fig. 2c), MGK and MGKZ-*x* possess nearly linear and symmetrical GCD curves. These demonstrate a highly reversible adsorption/desorption of electrolyte ions in the skeleton of MGKZ-*x*, especially in MGKZ-2. As shown in Fig. 2d and e, the specific capacitance of MGKZ-2 is as high as 353.8 F g^{-1} at 0.5 A g^{-1}. Even at 50 A g^{-1}, the specific capacitance (229 F g^{-1}) can still maintain 64.7% of its initial value. Notably, the specific capacitance of MGKZ-2 is higher than the other biomass-derived carbons (Table S2). The internal resistance of MGKZ-*x* electrodes is less than 1 Ω while the values of MG and MGK are around 1.9 Ω and 1.2 Ω (Fig. 2f), implying MGKZ-*x* have higher electrode conductivity than MG and MGK.

It is clear that the voltage window of rectangular CV curve for the MGKZ-2-based symmetric supercapacitor is maintained even at 1.6 V, demonstrating it can be reversibly cycled within the voltage window of 0–1.6 V (Fig. 3a). Furthermore, Fig. 3b reveal that the rectangular shape can be retained at different scan rates, indicating fast and efficient charge transfer. The linear and nearly symmetric GCD curves for the symmetric supercapacitor shown in Fig. 3c reveal good capacitive characteristic. The relatively low IR drop suggests the symmetric cell has low internal resistance due to fast charge transfer and ion diffusion [9]. As can be seen from Fig. 3d, when increasing the current density from 0.2 A g^{-1} to 10 A g^{-1}, a capacitance retention of 75.9% is obtained, indicating its excellent rate capability. The Nyquist plots of EIS tests for the symmetric supercapacitor are shown in Fig. 3e. The intercept (1.6 Ω) at the real axis, the small semicircle in the high-frequency region, and vertical-line feature in the low-frequency region indicate the charge transfer and ion diffusion speed are fast enough at the materials surface. The Ragone plot shown in Fig. 3f exhibits a high energy density of 27.6 Wh kg^{-1} at a power density of 159.9 W kg^{-1}. The capacitor demonstrates superior cycling durability after 10,000 cycles, and an excellent reversibility with a coulombic efficiency of nearly 100% for each charge/discharge process (Fig. 3g).

4. Conclusions

The carbon electrode materials with hierarchical pores for high-performance supercapacitor are facilely synthesized from bio waste-mango stone. The specific capacitance of the optimized MGKZ-2 reaches 353.8 F g^{-1} at 0.5 A g^{-1} and even retains 229.0 F g^{-1} at 50 A g^{-1}. Moreover, the MGKZ-2-based symmetric cell displays a high energy density of 27.6 Wh kg^{-1} at 159.9 W kg^{-1} and presents an excellent long-term cycling stability.

Acknowledgements

Financial supports from the National Natural Science Foundation of China (No. U1304203), the Foundation of Henan Educational Committee (No. 16A150046), the Natural Science Foundation of Henan Province (No. 162300410258), the College Science and Technology Innovation Team of Henan Province (No. 16IRTSTHN001) and the Innovation Foundation of Zhengzhou University (No. 201810459003) are greatly acknowledged.

Appendix A. Supplementary data

Supplementary data associated with this article can be found, in the online version, at https://doi.org/10.1016/j.matlet.2018.07.096.

References

[1] P. Simon, Y. Gogotsi, Materials for electrochemical capacitors, Nat. Mater. 7 (2008) 845–854.
[2] L.X. Shen, L.H. Du, S.Z. Tan, Z.G. Zang, C.X. Zhao, W.J. Mai, Flexible electrochromic supercapacitor hybrid electrodes based on tungsten oxide films and silver nanowires, Chem. Commun. 52 (2016) 6296–6299.
[3] C.L. Long, X. Chen, L.L. Jiang, L.J. Zhi, Z.J. Fan, Porous layer-stacking carbon derived from in-built template in biomass for high volumetric performance supercapacitors, Nano Energy 12 (2015) 141–151.
[4] J.Y. Huang, L.D. Chen, H.W. Dong, Y. Zeng, H. Hu, M.T. Zheng, Y.L. Liu, Y. Xiao, Y.R. Liang, Hierarchical porous carbon with network morphology derived from natural leaf for superior aqueous symmetrical supercapacitors, Electrochim. Acta 258 (2017) 504–511.
[5] E.C. Hao, W. Liu, S. Liu, Y. Zhang, H.L. Wang, S.G. Chen, F.L. Cheng, S.P. Zhao, H.Z. Yang, Rich sulfur doping porous carbon materials derived from ginkgo leaves for multiple electrochemical energy storage, J. Mater. Chem. A 5 (2017) 2204–2214.
[6] L.L. Jiang, L.Z. Sheng, C.L. Long, Z.J. Fan, Densely packed graphene nanomesh-carbon nanotube hybrid film for ultra-high volumetric performance supercapacitors, Nano Energy 11 (2015) 471–480.
[7] Y.J. Cai, Y. Luo, Y. Xiao, X. Zhao, Y.R. Liang, H. Hu, H.W. Dong, L.Y. Sun, Y.L. Liu, M. T. Zheng, Facile synthesis of three-dimensional heteroatom-doped and hierarchical egg-box-like carbons derived from moringa oleifera branches for high-performance supercapacitors, ACS Appl. Mater. Interfaces 48 (2016) 33060–33071.
[8] N.N. Guo, M. Li, Y. Wang, X.K. Sun, F. Wang, R. Yang, Soybean root-derived hierarchical porous carbon as electrode material for high-performance supercapacitors in ionic liquids, ACS Appl. Mater. Interfaces 8 (2016) 33626–33634.
[9] Y.J. Li, G.L. Wang, T. Wei, Z.J. Fan, P. Yan, Nitrogen and sulfur co-doped porous carbon nanosheets derived from willow catkin for supercapacitors, Nano Energy 19 (2016) 165–175.